BIOMIMETIC DEPOSITION OF APATITE ON SURFACE CHEMICALLY MODIFIED POROUS NiTi SHAPEMEMORY ALLOY

S.L. WU, X.M. LIU, C.Y. CHUNG*, PAUL K. CHU
Department of Physics & Materials Science, City University of Hong Kong, Tat Chee Avenue, Kowloon, Hong Kong
*appchung@cityu.edu.hk
Y.L. CHAN and K.W.K. YEUNG
Division of Spine Surgery, Department of Orthopaedics and Traumatology, The University of Hong Kong, Pokfulam, Hong Kong
C.L. CHU
School of Materials Science and Engineering, Southeast University, Nanjing 210018, China

Porous NiTi shape memory alloy (SMA) with 48% porosity and an average pore size of 50–800μm was synthesized by capsule-free hot isostatic pressing (CF-HIP). To enhance the surface bioactivity, the porous NiTi SMA was subjected to H_2O_2 and subsequent NaOH treatment. Scanning electron microscopy (SEM), X-ray diffraction (XRD), and X-ray photoelectron spectroscopy (XPS) analyses revealed that a porous sodium titanate (Na_2TiO_3) film had formed on the surface of the porous NiTi SMA. An apatite layer was deposited on this film after immersion in simulated body fluid (SBF) at 37°C, while no apatite could be found on the surface of the untreated porous NiTi SMA. The formation of the apatite layer infers that the bioactivity of the porous NiTi SMA may be enhanced by surface chemical treatment, which is favorable for its application as bone implants.

Keywords: Porous NiTi; Shape memory alloy; Surface modification; Apatite; Bioactivity; Biomimetic.

1. Introduction

Porous NiTi shape memory alloys (SMAs) from powder metallurgical (PM) methods have attracted considerable attentions in orthopedic fields as one of most promising biomaterials for hard tissue repair and reconstruction applications [1-4], which is due to its excellent superelasticity (SE), good mechanical properties and interconnected open porous structure. [1, 2, 5-9]. However, the high nickel content of NiTi alloys is of great concern affecting its biocompatibility because the released nickel ions was reported one of the causes for some allergic contact dermatitis and asthma. [10-12] The large exposed surface area of the porous structure makes porous alloy more susceptible to nickel-leaching than dense NiTi SMAs,[13] and the complex surface morphology makes it more difficult to modify the entire exposed surface of the porous NiTi SMAs by common line-of-sight PVD techniques. The development of non-line-of-sight methods,[5, 14-17] such as chemical treatment is needed.

Chemical treatments have been reported to be effective in modifying the surface of Ti and Ti-based alloys to favor the formation of bioactive apatite on the surface in simulated body fluids (SBF) and prevent nickel ions from leaching-out from the dense NiTi SMAs. [18-30] It is believed that this method is suitable for modifying the complex surface of porous NiTi due to its non-line-of-sight nature better than plasma immersion ion implantation (PIII) and air oxidation. [5, 16, 17] In chemical treatment, different chemical solutions such as hydrogen peroxide solution (H_2O_2), H_2SO_4 and NHO_3 were often used to pre-treat titanium metal to form a layer of titania film followed by alkaline treatment. [31-35] However, these reports focused on the enhancement of surface bioactivity of dense materials, and few studies were carried out on porous NiTi SMAs. The recent investigation of Jiang and Rong revealed that HNO_3 solution and subsequent NaOH treatment can enhance the formation of hydroxyapatite (HA) on the surface of porous NiTi immersed in SBF.[13] It also depressed nickel-leaching, and they ascribed the superior behavior to the formation of TiO_2 and $NaTiO_3$. However, there is no systematical analysis of the surface structure of the exposed

pores prior the formation of HA.

In this work, porous NiTi SMAs fabricated by capsule-free hot isostatic pressing (CF-HIP) were chemically pre-treated by H_2O_2 and subsequent NaOH treatment. The surface chemically modified NiTi SMAs were subsequently immersed in SBF for various periods of time to investigate their biomimetic apatite-forming ability. Scanning electron microscopy (SEM), small area X-ray photoelectron spectroscopy (XPS) were used to characterize the layer produced by chemical modification and the apatite formed in porous NiTi SMAs.

2. Experimental Details

Porous NiTi SMAs were fabricated using thoroughly mixed equiatomic Ni and Ti powders by capsule-free hot isostatic pressing. The mixed powders were compressed into a rod shape green compacts by a uniaxial hydraulic press. The green compact was hot isostatic pressing (HIP) chamber which was vacuumed and backfilled with pure argon. The argon pressure and temperature were then raised simultaneously to 150 MPa and 1050 ^oC respectively. The high pressure and temperature were kept for 3 hours allowing sufficient solid state diffusion of the nickel and titanium. Details of the CF-HIP process can be found in our previous publications.[36, 37] The porosity of the sample was about 48%, which was calculated using by the equation:

$$p = (1 - \rho/\rho_0) \times 100\%$$

Where ρ is the density of the porous NiTi SMAs (mass/the theoretical volume), ρ_0 is 6.45 g/cm^3 (the theoretical density) of NiTi SMAs. The open porosity was approximately 70%, which is determined according to the ASTM B328-96 protocol.[38] The pore size of porous NiTi SMAs was found in the range of 100– 600 μm. The samples used for chemical modification were cut into disks 6mm in diameter and 2mm thick from the porous NiTi SMAs. They were mechanically polished progressively from 240 to 800 grits sandpapers, ultrasonically cleaned with acetone and rinsed with de-ionized water before leaving to dry overnight in air at room temperature.

Before treatment, the samples were divided into two groups. The first group was used as control without treatment. The second group was oxidized for 4 hours in an 80^oC aqueous solution containing 30% H_2O_2, then ultrasonically rinsed with de-ionized water for 20min. Subsequently, these samples were treated in 10M NaOH aqueous solution at 60^oC for 24 hours, and finally ultrasonically cleaned and rinsed with de-ionized water for 20min. For the above treated and untreated samples, each sample was incubated in 25 ml of SBF with a pH value of 7.42 at 37±0.5^oC. The SBF composed of 7.996 g/l of NaCl, 0.35 g/l of $NaHCO_3$. 0.224 g/l of KCl, 0.228 g/l of $K_2HPO_4{\cdot}3H_2O$, 0.305 g/l of $MgCl_2{\cdot}6H_2O$, 0.278 g/l of $CaCl_2$, 0.071 g/l of Na_2SO_4, as well as 6.057 g/l $(CH_2OH)_3CNH_2$, with ionic concentrations similar to human body blood plasma.[39] After the samples were immersed for various periods of time, i.e. 5, 10 and 15 days, they were removed from the solution, gently rinsed with de-ionized water, and dried at room temperature. The nickel concentration in the corresponding SBF was measured using inductively-coupled plasma mass spectrometry (ICPMS) [Perkin Elmer, PE SCIEX ELAN6100, USA]. During the immersion tests, the SBF solution was not replenished.

The surface morphologies of the samples were examined using scanning electron microscope (SEM JSM820) equipped with an energy-dispersive spectroscopy (EDS). EDS was performed to determine the composition of the modified surface. A field emission scanning electron microscope (FESEM, JEOL JSM-6335F) was used examine the morphology of the bioactive layer. Thin film X-ray diffraction (TF-XRD) measurement was conducted using a Philips X'pert X-ray diffractomer (CuKα radiation, 40 kV, 30 mA, grazing incidence at 5^o). The data were collected in the 2θ range of 20 ^{o}–50 ^{o} with a step increment of 0.01^o. The chemical composition depth profile were determined by X-ray photoelectron spectroscopy (XPS) [Physical electronics PHI 5802, Minnesota, USA] using an aluminum X-ray source with a power of 350 W. The take-off angle was 45^o and the base vacuum was 2×10^{-8} Pa. Survey scans were first conducted to measure the elemental species on the surfaces over a binding energy range of 0-1400 eV in 0.8 eV steps using a pass energy of 187.85 eV. In order to determine the composition of the exposed surface, high resolution small area (120 μm) XPS analysis was performed on the wall of one of the internal pore using a pass energy of

11.75 eV and 0.1 eV step. A Gaussian-Lorentzian peak fitting model was used to deconvolute the special narrow scan spectra such as Na1s, O1s, Ti2p and Ni 2p.

3. Results and discussion

Fig. 1 (a) shows the typical surface morphology of porous NiTi SMA fabricated by CF-HIP. The size of most pores was in the range of 50-800μm and interconnected. This interconnected porous structure with big pore size allows the tissue in-growth and favors the fixation of bone implants. It can be found from Fig. 1(b) that, after oxidization in H_2O_2 solution, a rough layer of oxides with some micro-crack formed on the surface, which was confirmed by the XPS results. (Details will be discussed in the part of XPS Analysis.)After treatment in NaOH solution with H_2O_2 preoxidation, a layer of spiculate structure forms on the surface of porous NiTi SMA [shown in Fig. 1(c)]. High magnification FESEM image reveals that this layer is a porous film with homogeneous distributed nano pores [shown in Fig. 1 (d)]. After 5 days immersion in SBF at 37 ^{o}C, some precipitates were found on the surface with discontinuous distribution [Fig. 1 (e)]. The amount and size of these precipitates increased as the immersion time increased. After immersion in SBF at 37 ^{o}C for 15 days, the surface was almost completely covered by a layer of such precipitates [Fig. 1 (f)]. Higher magnification image revealed that there were small pores on the precipitated particles [Fig. 1 (g)].

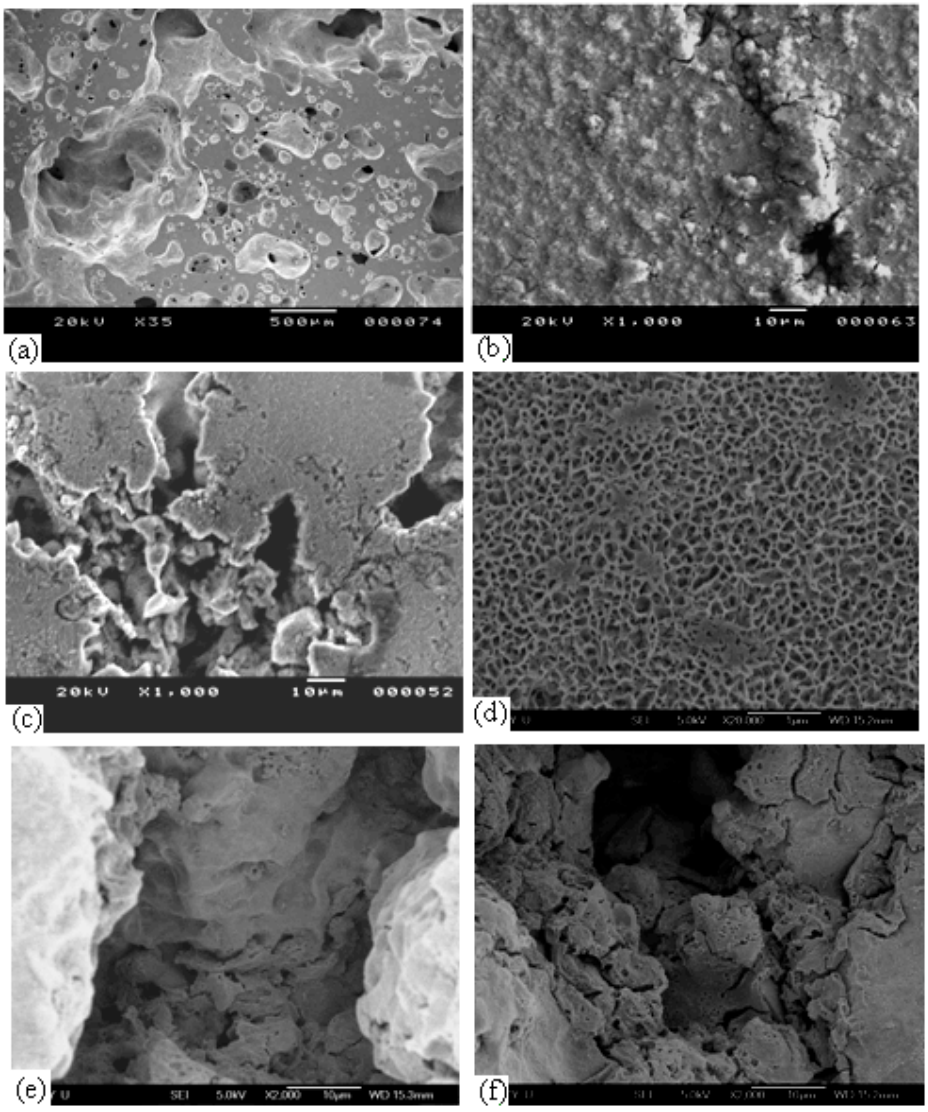

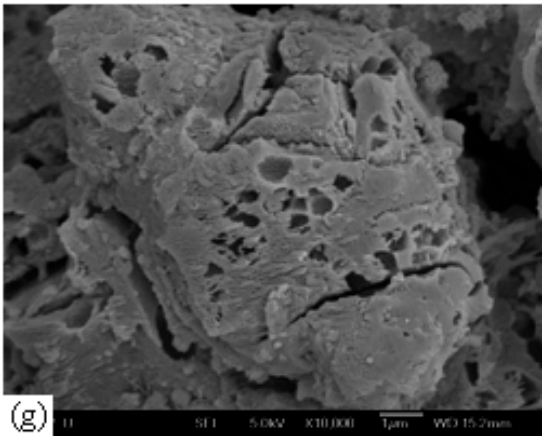

Fig. 1. Morphology of porous NiTi: (a) typical surface morphology of the untreated porous NiTi fabricated by capsule-free hot isostatic pressing; (b) after H_2O_2 aqueous treatment; (c) after H_2O_2 aqueous pretreatment and subsequent NaOH aqueous treatment; (d) high magnification image of (c); sample shown in (c) after immersion in SBF for (e) 5 days and (f) 15 days; (g) high magnification image of (f);

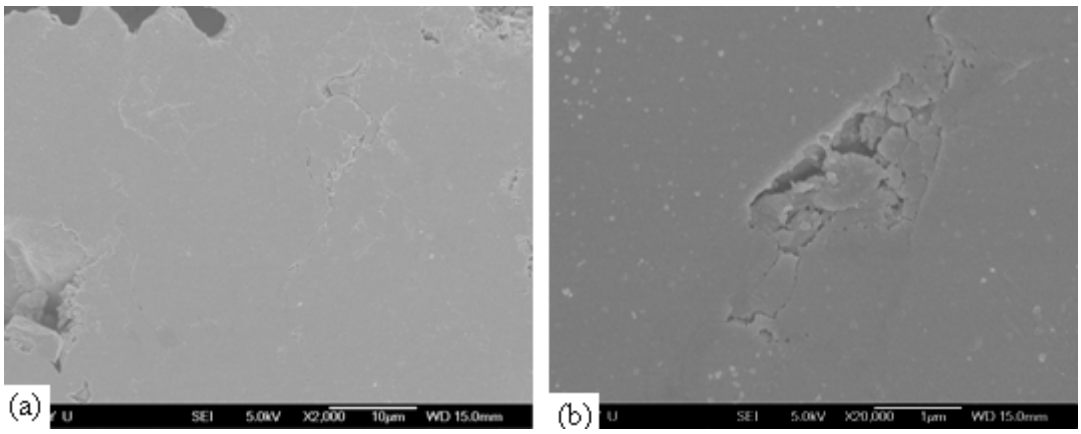

Fig. 2. Micrographs of the untreated porous NiTi SMA immersed in SBF (a) for 15 days; (b) high magnification image of (a);

In comparison, Figs.2 (a) and (b) shows the surface micrograph and the corresponding high magnification image of the untreated porous NiTi SMA immersed in SBF at 37 ^{o}C for 15 days. There was no precipitate found on the surface of the untreated porous sample, which reveals that Na_2TiO_3 (confirmed by EDS, XRD and XPS in the next parts) formed on porous NiTi alloy by chemically modification is bioactive and favor the formation of the bone-like apatite. The EDS results shown in Fig. 3 indicates that the precipitates contain calcium and phosphorous. The peaks of Na and O can also be detected. The signal of Ti and Ni should come from the NiTi alloy substrate. Fig. 4 shows the TF-XRD pattern of surface chemically modified porous NiTi immersed in SBF for 15 days at 37 ^{o}C. It was found that the precipitated layer mainly composed of apatite. Minor TiO_2 and Na_2TiO_3 exist on the surface layer, which could be the products of chemical reaction during the chemical modification process [13].

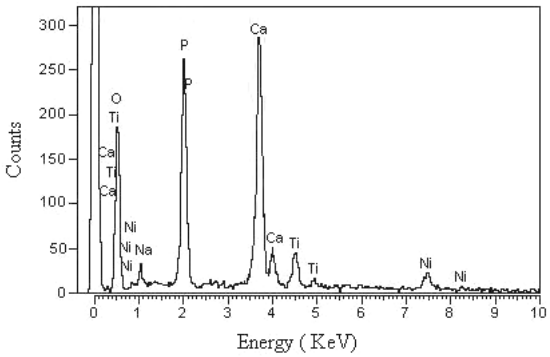

Fig. 3. SEM-EDS profile of the surface chemically modified porous NiTi alloy after immersed in SBF for 15 days;

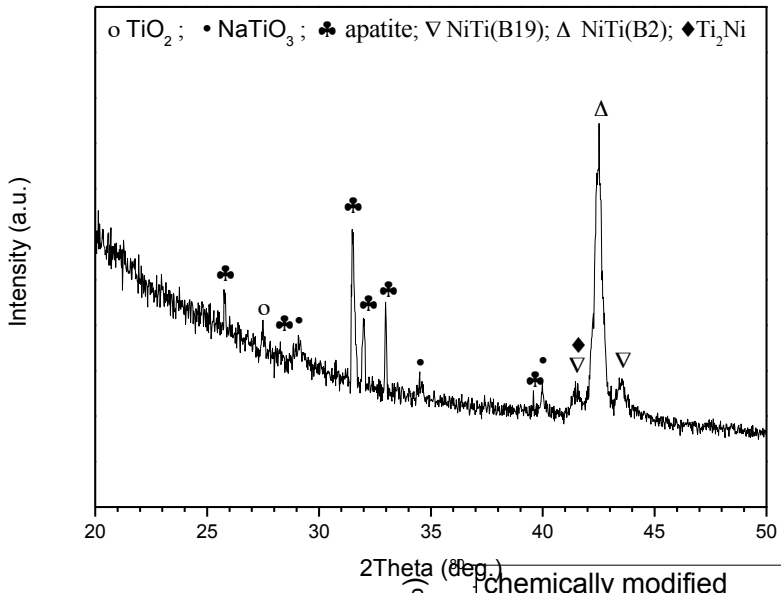

Fig. 4. TF-XRD pattern of the surface chemically modified porous NiTi immersed in SBF for 15 days at 37 °C.

Fig. 5 shows the XPS depth profiles of the untreated and surface chemically modified porous NiTi alloys. As shown in Fig. 5 (a), there exists a thin layer of oxides with thickness of several nm on the untreated porous NiTi. The oxides possibly come from the natural oxidation in air after mechanical polishing.

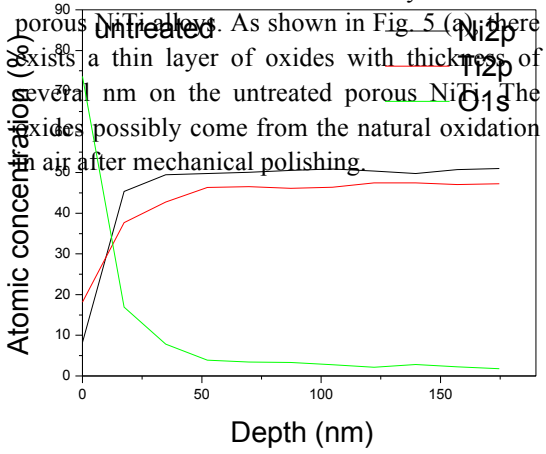

(a)

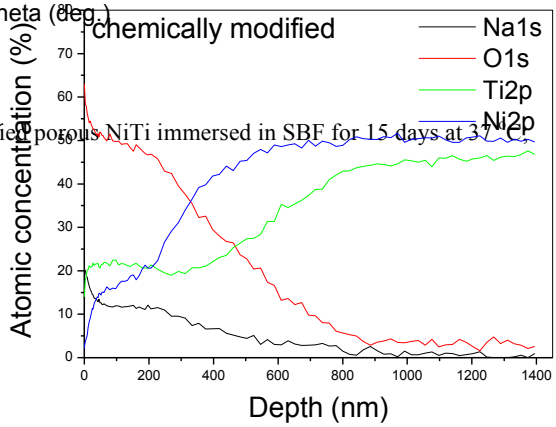

(b)

Fig. 5. XPS depth profile of the porous NiTi: (a) untreated sample; (b) surface chemically modified sample;

The high resolution XPS narrow spectra shown in Fig. 6 (a) reveals that this layer mainly composed of TiO_2, minor TiO and NiTi (according to the fitting curve of Ti2p spectra, not shown here) [5]. In comparison, for surface chemically modified porous NiTi, the thickness of the surface layer was about 800nm thick, which exhibits a graded structure [shown in Fig. 5 (b)].

Fig. 6 (b) shows the high resolution XPS narrow spectra of Ti2p of the surface chemically modified porous NiTi alloy. It is obvious that from the surface to the substrate, Ti2p3/2 exhibits three different binding energies of 458.3 eV, 459.1 eV and 454.5 eV, corresponding to the surface layer, the middle layer and the substrate, respectively. According to the reported binding energies of Ti2p3/2 in different compounds [40], Ti2p signal from the surface layer can be attributed to TiO_3^{2-}. In the middle layer, Ti2p should be due to TiO_2 and TiO_3^{2-} (according to the fitting curve of Ti2p spectra, not shown here). As the depth increases, the amount of TiO_2 and TiO_3^{2-} decrease while the amount of metal Ti (NiTi) increases.

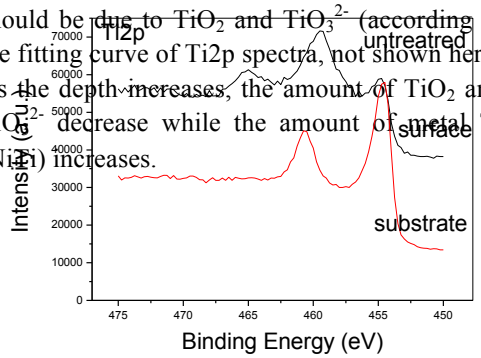

(a)

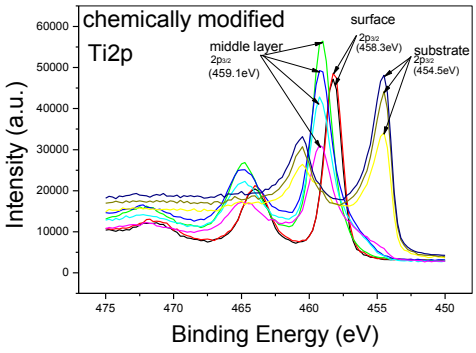

(b)

Fig. 6. High resolution XPS narrow spectra of Ti2p; (a) untreated sample; (b) surface chemically modified sample;

Combined with the depth profile curves shown in Fig. 5 (b), it was evident that the surface layer of surface chemically modified porous NiTi alloy was dominantly composed of Na_2TiO_3, while the middle layer composed of TiO_2, Na_2TiO_3 and trace amount of NiTi. The amount of TiO_2 and Na_2TiO_3 gradually decrease when it was closer to the substrate. Binding energy signals of NiTi dominate when the depth was more than 800 nm.

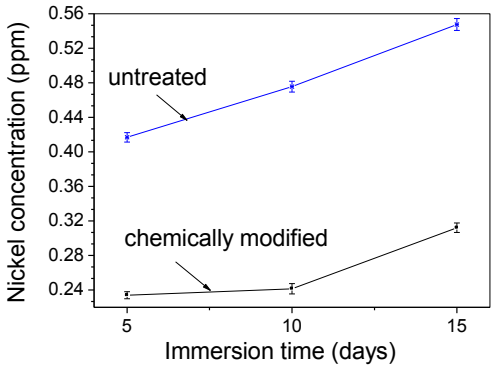

Fig. 7. Nickel release concentration of porous NiTi samples at different immersion duration in SBF.

The amount of nickel released from the untreated and surface chemically modified porous samples to the SBF for different time duration is shown in Fig. 7. For both of the untreated and surface chemically modified porous samples, the amount of nickel released increased when the immersion time increased. The nickel released from the surface chemically modified sample decreased significantly. This can be the effect of the 800 nm thick graded layer composed of Na_2TiO_3 and TiO_2 formed on the surface of porous NiTi alloy [shown in Fig 5(b)], which prevents the nickel leaching-out from the substrate. Furthermore, this graded layer can facilitate the nucleation and growth of apatite in SBF. The enhanced deposition of apatite also lead to more effective blocking of the nickel released from the NiTi substrate. For the untreated porous NiTi, there exist only several nm nature oxides on the surface.

4. Conclusions

A graded bioactive layer mainly composed of Na_2TiO_3 and TiO_2 can be prepared on the surface of porous NiTi SMA by H_2O_2 and subsequent NaOH treatment, which is favorable for the biomimetic deposition of bone-like apatite on the surface of porous NiTi alloy in SBF at 37 ^oC in comparison with the untreated porous sample. Furthermore, as a non-line-of-sight modification technique, chemical surface modification can also effectively hinder the nickel out leakage from porous NiTi alloys with

complex surface morphology and large exposed area.

Acknowledgements

This work was jointly supported by Hong Kong Research Grants Council (RGG) Central Allocation Group Research Grant No. CityU 1/04C, City University of Hong Kong Applied Research Grant No. 9667002 and the SRG grant from the Research Committee of the CityU of HK (Project #: 7001999).

References

1. Itin VI, Gyunter VE, Shabalovskaya SA, Sachdeva RLC. Mechanical properties and shape memory of porous nitinol. Mater Charact 1994; 32: 179.
2. Li BY, Rong LJ, Li YY, Gjunter VE. Synthesis of porous Ni-Ti shape-memory alloys by self-propagating high-temperature synthesis reaction mechanism and anisotropy in pore structure. Acta Mater 2000; 48: 3895
3. Silbersteinm BM, Gjunter VE. Shape-Memory Implants in Spinal Surgery, Springer, Berlin, 2000, p. 147.
4. Simske SJ, Sachdeva R. Cranial bone apposition and ingrowth in a porous nickel–titanium implant. J Biomed Mater Res 1995; 29: 527.
5. Wu SL, Chu PK, Liu XM, Chung CY, Ho JPY, Chu CL, Tjong SC, Yeung KWK, Lu WW, Cheung KMC, Luk KDK. Surface characteristics, mechanical properties, and cytocompatibility of oxygen plasma-implanted porous nickel titanium shape memory alloy. J Biomed Mater Res A 2006; 79: 139
6. Greiner C, Oppenheimer SM, Dunand DC. High strength, low stiffness, porous NiTi with superelastic properties. Acta Biomaterialia 2005; 1: 705.
7. Zhao Y, Taya M, Kang YS, Kawasaki A. Compression behavior of porous NiTi shape memory alloy. Acta Mater 2005; 53: 337.
8. Prymak O, Bogdanski D, Koller M, Esenwein SA, Muhr G, Beckmann F, Donath T, Assad M, Epple M. Morphological characterization and in vitro biocompatibility of a porous nickel-titanium alloy. Biomaterials 2005; 26: 5801
9. Chu CL, Chung CY, Lin PH, Wang SD. Fabrication and properties of porous NiTi shape memory alloys for heavy load-bearing medical applications. J Mater. Process Technol 2005; 169: 103
10. Peltonen L. Nickel sensitivity in the general population. Contact Dermatitis 1979; 5: 27.
11. Barrett RD, Bishara SE, Quinn JK. Biodegradation of orthodontic appliances. 1. biodegradation of nickel and chromium in vitro. Am. J. Orthod. Dentofac. Orthoped. 1993; 103: 8.
12. Rondelli G, Vicentini B. Bone modeling and cell–material interface responses induced by nickel–titan ium shape memory alloy after periosteal implantation. Biomaterials 1999; 20: 1309.
13. Jiang HC, Rong LJ. Effect of hydroxyapatite coating on nickel release of the porous NiTi shape memory alloy fabricated by SHS method, Surface & Coatings Technology 2006; 201: 1017.
14. Cui ZD, Man HC, Yang XJ. Characterization of the laser gas nitrided surface of NiTi shape memory alloy. Appl Surf Sci 2003; 208: 388.
15. Lotkov AI, Meisner LL, Grishkov VN. Titanium nickelide-based alloys: Surface modification with ion beams, plasma flows, and chemical treatment. Phys Met Metallogr 2005; 99: 508.
16. Wu SL, Liu XM, Chan YL, Ho J PY, Chung CY, Chu PK, Chu CL, Yeung KW K, Lu WW, Cheung KMC, Luk KDK, "Nickel Release Behavior, Cyto-Compatibility, and Superelasticity of Oxidized Porous Single-Phase NiTi", Journal of Biomedical Materials Research A (*in press*) 2007. DOI: 10.1002/jbm.a.31115
17. Gu YW, Tay BY, Lim CS, Yong MS. Biomimetic deposition of apatite coating on surface-modified NiTi alloy, Biomaterials 2005; 26: 6916.
18. Ken Nishio, Masashi Neo, Haruhiko Akiyama, Shigeru Nishiguchi, Hyun-Min Kim, Tadashi Kokubo, Takashi Nakamura. The effect of alkali- and heat-treated titanium and apatite-formed titanium on osteoblastic differentiation of bone marrow cells, J Biomed Mater Res 2000; 52: 652.
19. Yong Han, Tao Fu, Jian Lu, Kewei Xu. Characterization and stability of hydroxyapatite coatings prepared by an electrodeposition and alkaline-treatment process, Journal of Biomedical Materials Research 2001; 54: 96.
20. Wang XX, Hayakawa S, Tsuru K, Osaka A. A comparative study of *in vitro* apatite deposition on heat-, H_2O_2-, and NaOH-treated titanium surfaces, J Biomed Mater Res 2001; 54: 172.

21. Wang XX, Hayakawa S, Tsuru K, Osaka A. Improvement of the bioactivity of $H_2O_2/TaCl_5$-treated titanium after a subsequent heat treatment. J Biomed Mater Res 2000;52: 171.
22. Kokubo T, Miyaji F, Kim HM, Nakamura T. Spontaneous formation of bone-like apatite layer on chemically treated titanium metals. J Am Ceram Soc 1996; 79: 1127.
23. Wen HB, Liu Q, De Wijn JR, De Groot K. Preparation of bio-active microporous titanium surface by a new two-step chemical treatment. J Mater Sci: Mater Med 1998; 9: 121.
24. Ohtsuki C, Iida H, Hayakawa S, Osaka A. Bioactivity of titanium treated with hydrogen peroxide solution containing metal chlorides. J Biomed Mater Res 1997; 35: 39.
25. Kim HM, Miyaji F, Kokubo T, Nakamura T. Preparation of bioactive Ti and its alloys via simple chemical surface treatment. J Biomed Mater Res 1996; 32: 409.
26. Wen HB, De Wijn JR, Cui FZ, De Groot K. Preparation of bioactive Ti6Al4V surfaces by a simple method. Biomaterials 1998; 19: 215.
27. Chu CL, Chung CY, Zhou J, Pu YP, Lin P H. Fabrication and characteristics of bioactive sodium titanate/titania graded film on NiTi shape memory alloy. J Biomed Mater Res 2005; 75A: 595.
28. Miyazaki T, Kim HM, Miyaji F, Kokubo T, Kato H, Nakamura T. Bioactive tantalum metal prepared by NaOH treatment. J Biomed Mater Res 2000; 50: 35.
29. Chen MF, Yang XJ, Liu Y, Zhu SL, Cui ZD, Man HC, Study on the formation of an apatite layer on NiTi shape memory alloy using a chemical treatment method, Surf. Coat. Technol. 2003;173: 229
30. Shi P, Geng F, Cheng FT. Preparation of titania–hydroxyapatite coating on NiTi via a low-temperature route, Materials Letters 2006; 60: 1996.
31. Wen HB, de Wijin JR, Cui FZ, de Groot K. Preparation of calcium phosphate coatings on titanium implant materials by simple chemistry. J Biomed Mater Res 1998; 41: 227.
32. de Andrade MC, Filgueiras MRT, Ogasawara T. Nucleation and growth of hydroxyapatite on titanium pretreated in NaOH solution. Experiments and thermodynamic explanation. J Biomed Mater Res 1999;46:441.
33. Xiao F, Tsuru K, Hayakawa S, Osaka A. In vitro apatite deposition on titania film derived from chemical treatment of Ti substrates with an oxysulfate solution containing hydrogen peroxide at low temperature. Thin Solid Films 2003; 441: 271
34. Jonasova L, Muller FA, Helebrant A, Strnad J, Greil P. Biomimetic apatite formation on chemically treated titanium. Biomaterials 2004; 25: 1187.
35. Kim HM, Miyaji F, Kokubo T, Nishiguchi S, Nakamura T. Graded surface structure of bioactive titanium prepared by chemical treatment. J Biomed Mater Res 1999; 45: 100.
36. Wu SL, Liu XM, Chu PK, Chung CY, Chu CL, Yeung KWK. Phase transformation behaviour of porous NiTi alloys fabricated by capsule-free hot isostatic pressing, Journal of Alloys and Compounds, in press, DOI 10.1016/j.jallcom.2006.01.144.
37. Wu SL, Chung CY, Liu XM, Chu PK, Ho JPY, Chu CL, Chan YL, Yeung KWK, Lu WW, Cheung KMC, and Luk KDK. Pore formation mechanism and characterization of porous NiTi shape memory alloys synthesized by capsule-free hot isostatic pressing, Acta Mater (2007), doi:10.1016/j.actamat.2007.01.045
38. ASTM Standard B328-96 (Reapproved 2003). American Society for Testing and Materials, Philadelphia, PA, 2003
39. Kokubo T, Kushitani H, Sakka S, Kitsugi T, Yamamuro T. Solutions able to reproduce in-vivo surface-structure changes in bioactive glass-ceramic A-W. J Biomed Mater Res 1990; 24: 721.
40. Moulder JF, Stickle WF, Sobol PE, Bomben KD, Chastain J. Handbook of X-Ray Photoelectron Spectroscopy: A Reference Book of Standard Spectra for Identification and Interpretation of XPS Data. Minnesota: Perkin-Elmer, Physical Electronics Division; 1992.